

## Direct Observation of Spontaneous Weak Ferromagnetism in the Superconductor $\text{ErNi}_2\text{B}_2\text{C}$

S.-M. Choi\* and J.W. Lynn

*National Institute of Standards and Technology, Gaithersburg, Maryland 20899  
and University of Maryland, College Park, Maryland 20742*

D. Lopez and P.L. Gammel

*Bell Laboratories, Lucent Technologies, Murray Hill, New Jersey 07974*

P.C. Canfield and S.L. Bud'ko

*Ames Laboratory and Department of Physics and Astronomy, Iowa State University, Ames, Iowa 50011  
(Received 27 March 2001; published 15 August 2001)*

Neutron measurements show that superconducting  $\text{ErNi}_2\text{B}_2\text{C}$  ( $T_C = 11$  K) develops antiferromagnetic spin density wave magnetic order ( $T_N = 6$  K), which squares up with decreasing temperature yielding a series of higher-order magnetic Bragg peaks with *odd* harmonics. Below  $T_{\text{WFM}} = 2.3$  K where magnetization indicates a net moment develops, *even-order* Bragg peaks develop which low field ( $\sim 3$  Oe) polarized beam measurements show are magnetic in origin. The data directly demonstrate the existence of a net magnetization with a periodicity of  $20a$ , confirming the microscopic coexistence of spontaneous weak ferromagnetism with superconductivity.

DOI: 10.1103/PhysRevLett.87.107001

PACS numbers: 74.25.Ha, 74.70.Dd, 75.25.+z

The coexistence of magnetic order and superconductivity has had an interesting history. The first examples of true long range magnetic order coexisting with superconductivity were provided by the ternary Chevrel phase superconductors ( $\text{RMO}_6\text{S}_8$ ) and related ( $\text{RRh}_4\text{B}_4$ ) ( $R = \text{rare earth}$ ) compounds [1]. The magnetic ordering temperatures are all low ( $\sim 1$  K), and thus it was argued that electromagnetic (dipolar) interactions dominate the energetics of the magnetic system. Similar behavior is found for the rare earth ordering in the hole-doped cuprates, which exhibit similar very low ordering temperatures [2]. The first systems where exchange clearly dominates the magnetic energetics were provided by the electron-doped cuprates [2], followed by the borocarbides of central interest here [3–5]. Most recently a spin density wave has been observed in the single-layer *d*-wave superconductor  $\text{La}_2\text{CuO}_{4+x}$  at  $T_C = T_N = 42$  K [6], and long range order of the Ru spins has been found at 135 K in the hybrid cuprate ruthenate  $\text{RuSr}_2\text{GdCu}_2\text{O}_8$  [7,8]. Among these systems, the rare and interesting situation where ferromagnetic interactions are present has attracted special attention because of the competitive nature between the superconducting screening (Meissner effect) and the internally generated magnetic field. In the Chevrel phase-type materials this competition gives rise to long wavelength oscillatory magnetic states and/or reentrant superconductivity [9–11] predicted theoretically, while the possibility of more exotic behavior such as spontaneous vortex formation has been speculated [12]. There has then been particular attention given to the report that superconducting  $\text{ErNi}_2\text{B}_2\text{C}$  ( $T_C = 11$  K) develops a net magnetization below 2.3 K [13], well below the onset of long range spin density wave order at  $T_N = 6$  K. Here we report a comprehensive study of the magnetic order in this material both above and below the transition at

2.3 K, and directly demonstrate that this transition does indeed correspond to the development of a net atomic magnetization in zero applied field, which coexists with the superconductivity.

The neutron measurements were performed at the NIST Center for Neutron Research on a superconducting single crystal ( $T_C = 11$  K) of  $\text{ErNi}_2^{11}\text{B}_2\text{C}$  grown using a high-temperature flux method [14]. To avoid extinction effects a relatively small crystal  $1 \times 1 \times 3$  mm<sup>3</sup>, with the *b* axis along the longer length, was used. Unpolarized neutron measurements were taken on the BT-7 triple-axis spectrometer with the standard configuration of a double-crystal pyrolytic graphite monochromator and an incident wavelength of 2.465 Å, with a 26' collimator between the sample and a pyrolytic graphite analyzer. The BT-2 triple-axis spectrometer was used at a neutron wavelength of 2.359 Å for polarized measurements, employing a Heusler monochromator and analyzer. The collimation was 60'-40'-40'-open and the direction of the guide field of 2–3 Oe at the sample position was controlled by four coils mounted around the cryostat. Data were collected primarily in the (*h* 0 *l*) scattering plane.

$\text{ErNi}_2\text{B}_2\text{C}$  orders magnetically at 6 K into a transversely polarized spin density wave structure [15–17], with the modulation wave vector  $\delta$  along the *a* axis and the spins along the *b* direction (or equivalently with  $\delta$  along *b* and the spins parallel to the *a* axis [18]). A portion of a scan along the *a* axis is shown in Fig. 1 at three temperatures; data have been collected over the range of 0.01–4.50 in reduced wave vector. Below  $T_N$  the initial ordering is a simple spin density wave as shown in the schematic, with a modulation of  $\delta \cong 0.55a^*$  ( $a^* = 2\pi/a$ ). The *T* dependence of the fundamental peak intensity is shown in Fig. 2a, where we see that the ordering temperature

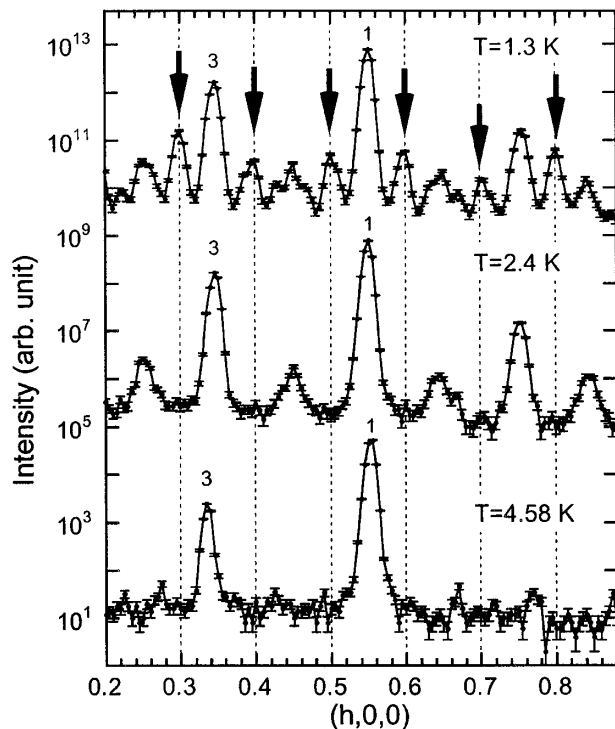


FIG. 1. Unpolarized neutron scattering measurements along  $(h, 0, 0)$  at  $T = 1.3, 2.4,$  and  $4.58$  K. The data have been offset for clarity. Above the weak ferromagnetic transition at  $2.3$  K we observe the fundamental peak at  $\sim 0.55$  along with odd-order harmonics, while below a new set of even harmonics develops (arrows). Also shown is a schematic of the spin density wave for  $T$  just below  $T_N$ , and the (undistorted) wave when it squares up.

is  $6.0$  K. The transition is also evident in the width of the scattering, which is resolution limited up to  $T_N$  and then broadens into critical scattering. The incommensurate wave vector  $\delta$  is  $T$  independent at low  $T$ , then exhibits a slight decrease before increasing with  $T$  up to  $T_N$ . Above  $T_N$  the average wave vector appears to decrease again.

At  $T = 4.58$  K (Fig. 1) we also observe a third-order peak at  $\sim 0.35a^*([2, 0, 0] - 3\delta)$ . The data are plotted on a log scale so that at this  $T$  the higher-order peak is quite small compared with the fundamental, but its presence indicates that the spin density wave has already begun to square up. At  $2.4$  K additional higher-order peaks become observable as the magnetic structure squares up as indicated schematically at the bottom of Fig. 1. The  $T$  dependence of the third-order peak (Fig. 2b) exhibits the expected concave upward curvature [17]. These peaks are all odd-order harmonics as expected for a square-wave

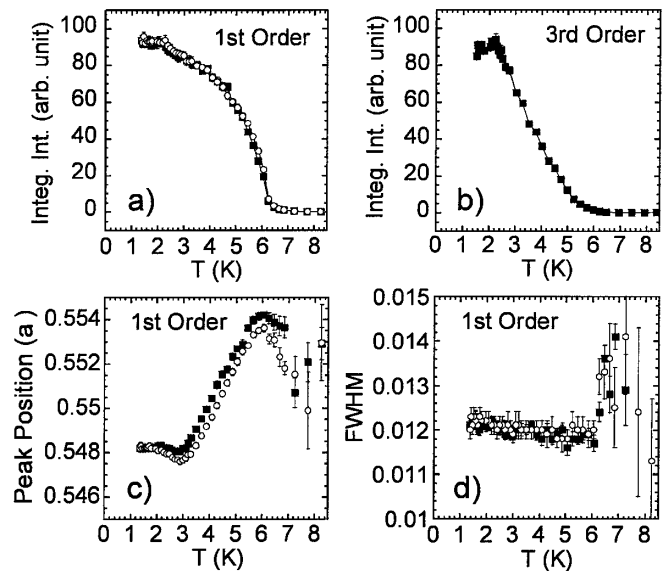


FIG. 2.  $T$  dependence of the intensity of the first (a) and third (b) harmonics of the spin density wave, along with (c) the position and (d) width of the fundamental. The solid squares are cooling and the open circles warming.

magnetic structure. The present results are in good agreement with previous work [15–17], while providing considerably more detail.

We now turn to the behavior of the magnetic system below the weak ferromagnetic transition ( $T_{WFM}$ ) at  $2.3$  K [13]. The low  $T$  diffraction data ( $T = 1.3$  K) shown in Fig. 1 indicate that a new series of peaks has developed, which are *even* harmonics of the fundamental wave vector. One possible origin for these new peaks is that the spin density wave couples to the lattice, producing an accompanying charge density wave distortion such as observed in Cr [19]; we have already noted that a small coupling that distorts the tetragonal lattice has been observed [18]. If such a distortion were the cause of the new peaks, then we would expect the odd-order peaks to be magnetic while the even-order peaks would be structural, and this can be unambiguously determined with polarized beam techniques [20]. Structural Bragg scattering never causes a reversal, or spin flip, of the neutron spin direction upon scattering. We denote this configuration as  $(\pm \pm)$ , where the neutron is incident with up (down) spin and remains in the up (down) state after scattering. The magnetic Bragg cross sections, on the other hand, depend on the relative orientation of the neutron polarization  $\mathbf{P}$ , the moment direction, and the reciprocal lattice vector  $\tau$ . For the  $(h 0 l)$  scattering plane the spin direction ( $b$ ) is vertical. Then when the neutron polarization is also vertical ( $\mathbf{P} \perp \tau$ ) the magnetic Bragg scattering is nonspin flip, while for  $\tau = (h, 0, 0)$  and ( $\mathbf{P} \parallel \tau$ ) the neutron spin is reversed  $[(- +) \text{ or } (+ -)]$  [20]. Figure 3 shows the scattering for an odd-order peak and an even-order peak that are conveniently located next to each other. All four cross sections are shown, and we see that the scattering for both types of peaks is spin flip for  $\mathbf{P} \parallel \tau$  and nonspin flip for  $\mathbf{P} \perp \tau$ . The ratio of the intensities

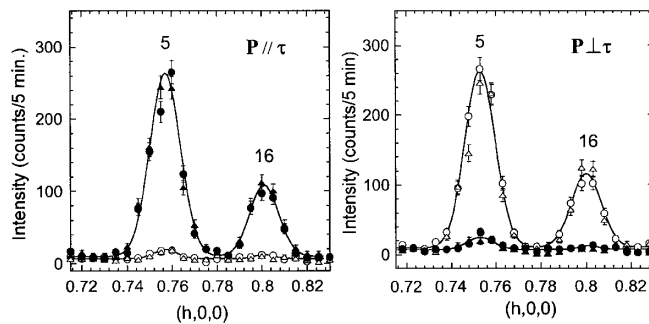


FIG. 3. Polarized neutron scattering measurements of the odd-order (5th) and even-order (16th) harmonics for the ( $\mathbf{P} \parallel \tau$ ) and ( $\mathbf{P} \perp \tau$ ) configurations. The solid circles ( $-$ ,  $+$ ) and solid triangles ( $+$ ,  $-$ ) are spin-flip scattering, while the open circles ( $+$ ,  $+$ ) and open triangles ( $-$ ,  $-$ ) are non-spin-flip scattering. The data demonstrate that both types of reflections are magnetic in origin, with the moment direction along the  $b$  axis.

was determined to be 24 for both peaks, which is the instrumental limit as measured at 15 K on the main Bragg peaks. It is therefore clear that both these peaks are magnetic in origin. Similar data have been obtained for all the higher-order harmonics observed in Fig. 1, and indicate that all the odd-order as well as the even-order (below  $T_{\text{WFM}}$ ) peaks are magnetic [21]. An important point to note in these measurements is that we have used a very small guide field, between 2 and 3 Oe, to control the neutron polarization. This is essential in determining the intrinsic zero-field behavior of the system, since applied fields above  $H_{C1}$  will not only strongly distort the magnetic state, but will induce vortices in the superconductor that will be coupled to the magnetic order [22]. The present results rule out the possibility that a charge density wave is the origin of the observed zero-field even-order peaks.

The integrated intensities of the odd- and even-order harmonics are shown in Fig. 4a as a function of  $T$ . The 5th harmonic increases with decreasing  $T$ , and then decreases again in intensity as the even-order peaks abruptly develop below 2.3 K. We therefore identify the even-

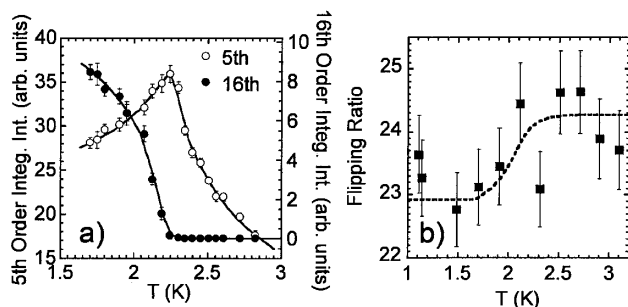


FIG. 4. (a) Integrated intensities of the odd-order (open circles) and even-order (solid circles) harmonics as a function of  $T$ . (b) Flipping ratio  $[I(++)]/I(+)]$  of the  $(0,0,2)$  peak, whose intensity is dominated by the strong nuclear scattering, across the weak ferromagnetic transition. The average (flat portions of the dashed curve) clearly decreases below  $T_{\text{WFM}}$ , indicating a ferromagnetic moment has developed.

order peaks with the development of weak ferromagnetism at  $T_{\text{WFM}} = 2.3$  K. There is also substantial thermal hysteresis associated with the weak ferromagnetic transition, with the odd- and even-order harmonics having the opposite type of behavior, suggesting that this transition is first order in nature. Hysteresis associated with  $T_{\text{WFM}}$  is also evident in  $\delta$  (Fig. 2c).

Finally, in addition to all the even-order components [2, 4, 6, ..., 16 (Fig. 3), 18, ...], there should be a zero-order component which sits on top of the strong nuclear Bragg reflection. To observe this component polarized beam measurements are necessary [23], and combined with the strong nuclear intensities the magnetic component is very difficult to observe. Nevertheless, in Fig. 4b we show the ratio of the  $(++)$  intensity to the  $(+-)$  intensity for the  $(0,0,2)$  Bragg peak, with ( $\mathbf{P} \perp \tau$ ) and a 2 Oe guide field [23]. The ratio of these intensities is observed to be  $T$  independent from 15 to  $\sim 2.3$  K, while with further decrease of  $T$  we observe a decrease in the ratio; the flat portions of the dashed curve indicate the average flipping ratio, which unambiguously decreases below  $T_{\text{WFM}}$ . Hence a (zeroth-order) *ferromagnetic* component has indeed developed below  $T_{\text{WFM}}$ .

The incommensurate spin density wave that forms in this system is controlled to a large extent by band structure (Fermi surface) effects [24]. For a localized  $4f$ -moment spin density wave, the magnetic structure must either square up at low  $T$ , or lock-in to a commensurate structure. The  $T$  dependence of  $\delta$  (Fig. 2c) clearly shows that there is no lock-in transition evident (in terms of a ratio of small integers) at this precision of measurement. It is also evident from the magnetic structure (Fig. 1) that there appears to be two different waves in the system. One is the short-period antiferromagnet just discussed, while the second one is a much longer period and describes the modulation away from this simple commensurate state; for  $\delta = 0.55$  this second period is  $\delta - 1/2 = 0.05$  or  $20a$  [17]. For this particular wave, every tenth spin will be forced to be parallel to its neighbor rather than antiferromagnetic. For the sinusoidal wave the system can arrange for this to occur at the place where the ordered moment is small, but when the wave squares up this becomes energetically unfavorable. For the actual system  $\delta$  is incommensurate, and when the wave becomes sufficiently square some energy can be saved by periodically disrupting the square wave with a discommensuration (or spin slip) [25] that locks it to the lattice by flipping one of the spins. The periodicity for this "mistake" is  $20a$ , which results in *even* harmonics (as well as changes to the odd-harmonic intensities) and a net magnetization  $2\mu_{\text{Er}}/20 \approx 0.7\mu_B$  parallel to  $(0,1,0)$ , i.e., to *spontaneous weak ferromagnetism* as has been observed via magnetization [13]. In the present case the intensities of the even-order peaks (including Fig. 4b) indicate a net moment/ $\text{Er}$  of  $(0.57 \pm 0.1)\mu_B$ . This is larger than the value obtained from the magnetization measurements, and may indicate that the bulk value is reduced due to superconducting screening effects.

The present neutron results demonstrate that a net magnetization develops in  $\text{ErNi}_2\text{B}_2\text{C}$  in the magnetically ordered state at low  $T$ , making this the first such “ferromagnetic superconductor” since  $\text{HoMo}_6\text{S}_8$  [10],  $\text{HoMo}_6\text{Se}_8$  [11], and  $\text{ErRh}_4\text{B}_4$  [9]. For  $\text{ErNi}_2\text{B}_2\text{C}$  the net magnetization is much smaller than for the above systems since just one in twenty moments is aligned, which allows coexistence with superconductivity over an extended  $T$  range. One of the advantages of the borocarbide materials is the ready availability of high quality single crystals, which has allowed an in-depth understanding of the magnetic structure and its interaction with the superconducting state. A similar net magnetization appears to develop [7] at the onset of antiferromagnetic order [8] in  $\text{RuSr}_2\text{GdCu}_2\text{O}_8$ , and it will be interesting to investigate this system in the same detail when single crystals become available. Finally we note that very recently superconductivity has been found with applied pressure in the itinerant electron ferromagnet  $\text{UGe}_2$ , with a comparable net moment in the coexistence regime [26]. The superconductivity in  $\text{UGe}_2$  appears to be of the spin-triplet form rather than the spin-singlet form for the above systems, thus providing a different but interesting type of competition between these two types of cooperative phenomena.

We thank C. M. Varma for helpful discussions. S.-M. C. and J. W. L. acknowledge support from the NSF, DMR-99-86442 and DMR 97-01339. P. C. C. and S. L. B. acknowledge support from the U.S.D.O.E., W-7405-Eng-82 and the Office of Basic Energy Sciences.

---

\*Present address: Department of Nuclear Engineering, Korea Advanced Institute of Science and Technology, Taejon, 305-701, Korea.

- [1] *Topics in Current Physics*, edited by Ø. Fischer and M. B. Maple (Springer-Verlag, New York, 1983), Vols. 32 and 34.
- [2] For a recent review, see J. W. Lynn and S. Skanthakumar, in *Handbook on the Physics and Chemistry of Rare Earths*, edited by K. A. Gschneidner, Jr., L. Eyring, and M. B. Maple (North Holland, Amsterdam, 2001), Vol. 31, Chap. 199, p. 313.
- [3] R. Nagarajan, C. Mazumdar, Z. Hossain, S. K. Dhar, K. V. Gopalakrishnan, L. C. Gupta, C. Godart, B. D. Padalia, and R. Vijayaraghavan, *Phys. Rev. Lett.* **72**, 274 (1994).
- [4] R. J. Cava, H. Takagi, B. Batlogg, H. W. Zandbergen, J. J. Krajewski, W. F. Peck, Jr., R. B. van Dover, R. J. Felder, T. Siegrist, K. Mizuhahi, J. O. Lee, H. Elsaki, S. A. Carter, and S. Uchida, *Nature (London)* **367**, 146 (1994).
- [5] P. C. Canfield, P. L. Gammel, and D. J. Bishop, *Phys. Today* **51**, No. 10, 40 (1998).
- [6] Y. S. Lee, R. J. Birgeneau, M. A. Kastner, Y. Endoh, S. Wakimoto, R. W. Erwin, S.-H. Lee, and G. Shirane, *Phys. Rev. B* **60**, 3643 (1999).
- [7] C. Bernhard, J. L. Tallon, Ch. Niedermayer, Th. Blasius, A. Golnik, E. Brücher, R. K. Kremer, D. R. Noakes, C. E. Stronach, and E. J. Ansaldo, *Phys. Rev. B* **59**, 14099 (1999).
- [8] J. W. Lynn, B. Keimer, C. Ulrich, C. Bernhard, and J. L. Tallon, *Phys. Rev. B* **61**, R14964 (2000).
- [9] D. E. Moncton, D. B. McWhan, P. H. Schmidt, G. Shirane, W. Thomlinson, M. B. Maple, H. B. MacKay, L. D. Woolf, Z. Fisk, and D. C. Johnston, *Phys. Rev. Lett.* **45**, 2060 (1980); S. K. Sinha, G. W. Crabtree, D. G. Hinks, and H. A. Mook, *Phys. Rev. Lett.* **48**, 950 (1982).
- [10] J. W. Lynn, D. E. Moncton, W. Thomlinson, G. Shirane, and R. N. Shelton, *Solid State Commun.* **26**, 493 (1978); J. W. Lynn, G. Shirane, W. Thomlinson, and R. N. Shelton, *Phys. Rev. Lett.* **46**, 368 (1981).
- [11] J. W. Lynn, J. A. Gotaas, R. W. Erwin, R. A. Ferrell, J. K. Bhattacharjee, R. N. Shelton, and P. Klavins, *Phys. Rev. Lett.* **52**, 133 (1984).
- [12] E. I. Blount and C. M. Varma, *Phys. Rev. Lett.* **42**, 1079 (1979); T. K. Ng and C. M. Varma, *Phys. Rev. B* **58**, 11624 (1998).
- [13] P. C. Canfield, S. L. Bud'ko, and B. K. Cho, *Physica (Amsterdam)* **262C**, 249 (1996).
- [14] B. K. Cho, P. C. Canfield, L. L. Miller, D. C. Johnston, W. P. Beyermann, and A. Yatskar, *Phys. Rev. B* **52**, 3684 (1995).
- [15] J. Zarestky, C. Stassis, A. I. Goldman, P. C. Canfield, P. Dervenagas, B. K. Cho, and D. C. Johnston, *Phys. Rev. B* **51**, 678 (1995).
- [16] S. K. Sinha, J. W. Lynn, T. E. Grigereit, Z. Hossain, L. C. Gupta, R. Nagarajan, and C. Godart, *Phys. Rev. B* **51**, 681 (1995).
- [17] J. W. Lynn, S. Skanthakumar, Q. Huang, S. K. Sinha, Z. Hossain, L. C. Gupta, R. Nagarajan, and C. Godart, *Phys. Rev. B* **55**, 6584 (1997).
- [18] There is a very small orthorhombic distortion that develops at the magnetic transition, indicating a small coupling to the lattice. The present sample then has multidomains, with average tetragonal symmetry. See C. Detlefs *et al.*, *Phys. Rev. B* **56**, 7843 (1997); C. Detlefs, D. L. Abernathy, G. Grubel, and P. C. Canfield, *Europhys. Lett.* **47**, 352 (1999).
- [19] E. Fawcett, *Rev. Mod. Phys.* **60**, 209 (1988).
- [20] R. M. Moon, T. Riste, and W. C. Koehler, *Phys. Rev.* **181**, 920 (1969).
- [21] It is possible that there is a small charge density wave distortion that accompanies the spin density wave, which might be revealed in x-ray measurements. There should also be a spin density wave in the conduction electrons that mediate the exchange interaction, which would be very interesting to observe. However, the magnetic scattering here is dominated by the localized Er 4f moment.
- [22] P. L. Gammel, B. P. Barber, A. P. Ramirez, C. M. Varma, D. J. Bishop, P. C. Canfield, V. G. Kogan, M. R. Eskildsen, N. H. Andersen, K. Mortensen, and K. Harada, *Phys. Rev. Lett.* **82**, 1756 (1999); S. L. Bud'ko and P. C. Canfield, *Phys. Rev. B* **61**, R14932 (2000).
- [23] The structural peaks have a significant  $T$  dependence below  $T_N$ , which make polarized beam techniques necessary to separate the magnetic and structural contributions. See H. Kawano, H. Tkeya, H. Yoshizawa, and K. Kadowaki, *J. Phys. Chem. Solids* **60**, 1053 (1999).
- [24] J. Y. Rhee, X. Wang, and B. N. Harmon, *Phys. Rev. B* **51**, 15585 (1995).
- [25] W. L. McMillan, *Phys. Rev. B* **14**, 1496 (1976). See also D. Gibbs, D. E. Moncton, K. L. D'Amico, J. Bohr, and B. H. Grier, *Phys. Rev. Lett.* **55**, 234 (1985).
- [26] S. S. Saxena *et al.*, *Science* **406**, 587 (2000).